Humic Acid Induces Oxidative DNA Damage, Growth Retardation, and Apoptosis in Human Primary Fibroblasts

MEI-LING CHENG,* HUNG-YAO HO,*,† YI-WEN HUANG,* FUNG-JOU LU,§ AND DANIEL TSUN-YEE CHIU*,[1]

*Graduate Institute of Medical Biotechnology and School of Medical Technology, Chang Gung University, Kwei-san, Tao-yuan, Taiwan; †Ronald O. Perelman Department of Dermatology, New York University School of Medicine, New York, New York 10016; and §Department of Biochemistry and Internal Medicine, College of Medicine, National Taiwan University, Taipei, Taiwan

Humic acid (HA) has been implicated as an etiological factor of Blackfoot disease endemic in the southwest coast of Taiwan. Dysfunction of endothelial cells and vasculopathy have been proposed to explain the onset of ulcerous changes at extremities. However, little is known about the effect of HA on activities of cells in these nonhealing wounds. In the present study, we demonstrate that HA adversely affects the growth properties of fibroblasts, one of the key players in wound repair. HA treatment caused growth arrest and apoptosis in human foreskin fibroblasts (HFF). This was accompanied by a significant increase in the level of 8-hydroxy-2'-deoxyguanosine (8-OHdG) in cellular DNA. The increased fluorescence in dichlorofluorescin (H_2DCF)-stained and HA-treated cells suggests the involvement of reactive oxygen species (ROS) in HA-induced biological effects. Conversely, vitamin E pretreatment, which significantly reduced the 8-OHdG formation in HA-treated cells, alleviated the growth-inhibitory and apoptosis-inducing effects of HA. These results indicate that HA initiates oxidative damages to fibroblasts, and leads to their dwindling growth potential and survival. The present study suggests that HA-induced growth retardation and apoptosis of fibroblasts may play a role in the pathogenesis of Blackfoot disease. Exp Biol Med 228:413–423, 2003

Key words: DNA damage; growth arrest; apoptosis; humic acid; 8-OHdG; ROS; vitamin E

This study was supported by the National Science Council Grants NSC 90-2320-B182-029 and NSC 89-2314-B182-069 and by Chang Gung Memorial Hospital Grants CMRP1048 and CMRP1024.
M.-L.C. and H.-Y.H. contributed equally to this paper.
[1] To whom requests for reprints should be addressed at Graduate Institute of Medical Biotechnology and School of Medical Technology, Chang Gung University, 259 Wen-Hua 1st Road, Kwei-san, Tao-yuan, Taiwan. E-mail: drychiu@mail.cgu.edu.tw

Received June 20, 2002.
Accepted December 11, 2002.

1535-3702/03/2284-0413$15.00
Copyright © 2003 by the Society for Experimental Biology and Medicine

Humic acid (HA) is a group of high-molecular-weight polymers that result from decomposition of organic matter, particularly dead plants. It exists abundantly in peat, soil, well water, and other sources (1). It consists of a mixture of closely related complex aromatic polymers, the exact composition of which varies with HA from different geographic locations. Chemical and infrared spectroscopic analyses revealed the presence of aromatic rings, phenolic hydroxyl, ketone carbonyl, quinone carbonyl, carboxyl, and alkoxyl groups in HA (2). A hypothetical "type" structure has been proposed: a polymer is composed of aromatic rings of the di- and trihydroxybenzene type that are bridged by ether, methylene, amine, imine, and other linkages; it also contains quinone groups and a variety of functional groups mentioned earlier (2–5).

HA was implicated as a causal factor of goiter (6–8), cancer (9), Blackfoot disease, an endemic peripheral vascular disease prevailing in the southwest coast of Taiwan (10–12), and Kashin-Beck disease, a chronic osteoarthritic disorder with necrosis of chondrocytes prevailing in mainland China (13). Epidemiologic and geochemical studies disclosed the presence of a high concentration of HA (approximately 200 ppm) in artesian well water from areas of endemic Blackfoot disease. The daily intake by an average resident in these regions was estimated to be as high as 400 mg (14, 15). Radioisotope tracing with iodinated HA in animals indicated that up to 60% of HA was retained in the body 24 hr after administration (16). It is believed that the intake of a huge amount of HA compromises the health of inhabitants, leading to the pathogenesis of Blackfoot disease.

Blackfoot disease begins with numbness or coldness, and can eventually proceed to black discoloration, ulceration, or gangrenous change in the extremities of patients. In pathology, Blackfoot disease is considered an arteriosclerotic disease (17, 18). Pathologic changes in blood vessels, such as mural thickening and accretion of subintimal

plaque, account for an impaired peripheral circulation, ischemia, and the onset of ulceration in extremities. Thrombosis, embolism, superimposed infection and/or alterations in blood viscosity, and blood cell deformability may aggravate such pathologic changes (19, 20). Most studies have been focused on interactions between HA and endothelial cells, which normally protect the vessels from atherogenesis and aberrant thrombus formation (21, 22). However, this is not a complete picture for ulcer, which also reflects an inability to self-repair in an orderly manner. The normal course of wound repair involves a cascade of well-orchestrated events, starting with hemostasis, proceeding through a delimited inflammatory stage, granulation tissue formation, and re-epithelialization. followed by scar formation and remodeling (23). In the ulcer, the wound remains in the inflammatory stage, and the healing process does not set in.

Fibroblast is a critical player in the formation of granulation tissue. Apart from producing such extracellular matrix constituents as collagen, elastin, and glycosaminoglycans, fibroblasts also secrete a number of mitogenic and chemotactic cytokines for keratinocytes, endothelial cells, and themselves (23, 24). Additionally, they act as cellular stitch: fibroblasts can change into a less proliferative and more contractile form known as myofibroblasts (25); these cells express smooth muscle contractile proteins, such as α-smooth muscle actin, and can generate forces necessary for wound contraction (26, 27). Any dysfunction of fibroblasts may pose difficulty for a chronic ulcer to heal. It is plausible that HA may induce damage of fibroblasts, contributing to the persistence of ulcers in Blackfoot patients.

In this article, we show that HA caused growth arrest and apoptosis in human foreskin fibroblasts. The level of 8-hydroxy-2'-deoxyguanosine (8-OHdG), a *de facto* marker of oxidative damage to genomic DNA (28–30), was significantly elevated after HA treatment. Increased fluorescence was observed in dichlorofluorescin (H_2DCF)-stained, HA-treated cells. Vitamin E, which greatly lessened the HA-induced damage to DNA, also protected the cells from growth inhibition and apoptosis-inducing effects of HA. These results demonstrate that HA acts via an oxidative mechanism. Taken together, the present study implies that HA-induced dysfunction of fibroblasts may play a role in the pathogenesis of Blackfoot disease.

Methods

Chemicals. Unless stated otherwise, all of the chemicals were obtained from Sigma (St. Louis, MO). Dulbecco's modified Eagle's medium (DMEM), fetal calf serum (FCS), penicillin, streptomycin, amphotericin, and trypan blue were purchased from GIBCO-Life Technology (Gaithersburg, MD). HA (sodium salt, technical grade) was obtained from Aldrich Chemical (Milwaukee, WI). Dichlorofluorescin diacetate (H_2DCFDA) was available through Molecular Probes (Eugene, OR). Antibodies to Rb (14001A), $p21^{Cip1}$ (C24420), and $p27^{Kip1}$ (K25020) were obtained from BD PharMingen (San Diego, CA); the anti-actin antibody (SC1615) was obtained from Santa Cruz Biotechnologies (Santa Cruz, CA). 8-OHdG and 2'-deoxyguanosine (dG) were purchased from Sigma. Nuclease P1 and alkaline phosphatase were obtained from Roche (Mannheim, Germany).

Purification of Aldrich HA. All of the experiments were performed with the same batch of HA purified from the one commercially available through Aldrich. Our purification method was similar to that described by Schnitzer (31) and is given below. The HA from Aldrich was first dissolved in 0.1 *N* NaOH solution, and any undissolved material was removed by centrifugation. The pH of supernatant was adjusted to 1.0 with 1 *N* HCl. Any precipitate formed was collected by centrifugation at 10,000*g* for 30 min, and was redissolved in 0.1 *N* NaOH. Such procedure of alkaline-acid treatment was repeated thrice. After the third round of acid precipitation, the precipitate was dissolved in 0.1 *N* NaOH, and pH of the resultant solution was adjusted to 7.2–7.4. It was then passed through the Sephadex G-25 column, and HA was eluted with distilled water. Elution profile was monitored by UV detector. Fractions corresponding to the first peak was collected, concentrated, and dried with a rotavapor. The HA was stored as dried powder, and was dissolved in phosphate-buffered saline (PBS) or water before experiments.

Cell Culture. Primary human foreskin fibroblasts were isolated as described elsewhere (32, 33). They were cultured in DMEM supplemented with 10% FCS, 100 units/ml penicillin, 100 units/ml streptomycin, and 0.25 mg/ml amphotericin at 37°C in a humidified atmosphere of 5% CO_2. The cells were fed every other day and were passaged at a ratio of 1:6 before the cultures were confluent. The cell number was determined by the trypan blue dye exclusion method.

Flow Cytometric Analysis of Cell Cycle. Cells were rinsed with ice-cold PBS, trypsinized, and resuspended in 0.3 ml of PBS. They were then fixed and permeabilized by addition of 0.7 ml of ethanol. After a brief wash, the cells were gently resuspended in 1 ml of propidium iodide (PI) stain solution (40 μg/ml propidium iodide, 100 μg/ml RNase A, and 0.5% Triton X-100 in PBS), and were incubated at room temperature for 30 min before analysis on a FACSCAN flow cytometer (Becton Dickinson, Mountain View, CA). The sub-G1 fraction is considered as the apoptotic cells and taken as a measure of the extent of apoptosis (34). The sub-G1 phase was quantified using *Modfit* software (Becton Dickinson).

Terminal dUTP Nick End (TUNEL) Labeling. TUNEL was performed with *in situ* cell death detection kit (Roche) according to the instructions of the manufacturer. In brief, the cells were trypsinized, washed with PBS, and resuspended in PBS. The cells (about 1×10^6 cells in 100 μl) were then fixed at room temperature for 1 hr by adding an equal volume of fixative solution (4% paraformaldehyde in PBS). The cells were washed, and then resuspended in permeabilization solution (0.1% Triton X-100 in 0.1% sodium citrate) at 4°C for 2 min. The sample was

washed twice with PBS, resuspended in 50 μl of TUNEL label solution, and incubated at 37°C for 1 hr. Finally, the cells were washed, resuspended in 500 μl of PBS, and analyzed by flow cytometry. The TUNEL-positive fraction was quantified by CellQuest software (Becton Dickinson) (33).

Detection of Reactive Oxygen Species (ROS) by H_2DCF Staining. Formation of ROS in cells was detected by monitoring the fluorescence of dichlorofluorescein (DCF), the oxidation product of H_2DCF, or that of rhodamine, the oxidation product of dihydrorhodamine 123 (DHR 123) (35, 36). The cells were loaded with 10 μ*M* dichlorofluorescin diacetate (H_2DCFDA) or DHR 123 for 5 min at 37°C. After treatment, they were immediately refed with fresh medium and observed under fluorescence microscope.

Ratio of 8-OHdG to dG. DNA was extracted from untreated or treated cells as described elsewhere (37). The DNA was dissolved in 200 μl of 20 m*M* sodium acetate (pH 5.2), digested to nucleotide level with 20 units of nuclease P1 at 37°C for 2 hr, and followed by treatment with 6 units of alkaline phosphatase in 20 m*M* Tris buffer (pH 8.5) at 37°C for 1.5 hr. The hydrolysate was filtered through microcon YM-10 (Millipore, Bedford, MA) before HPLC analysis to remove enzymes and other macromolecules. Nucleosides in the filtrate were separated by a reverse-phase high-performance liquid chromatography (HPLC) system (ESA, Inc., Chelmsford, MA) equipped with a C8 column (3 μm, 4.6 × 150 mm, YMC-BD), and eluted at a flow rate of 1.0 ml/min with the mobile phase of 5% methanol in 100 m*M* sodium acetate buffer (pH 5.2) (38). The 8-OHdG and dG were monitored with an ESA Coulochem II electrochemical detector; the high sensitivity analytical cell 5010 were set at 150 mV for electrode 1, 300 mV for electrode 2 (with a full range deflection of 100 nA), 700 mV for electrode 3, and 800 mV for electrode 4 (with a full range deflection of 100 μA), respectively. The amounts of 8-OHdG and dG were quantified with respect to standards. The 8-OHdG levels are expressed as the number of 8-OHdG molecules per 10^6 dG.

Western Blotting. The cells were rinsed with cold PBS, scraped, and collected by centrifugation. They were immediately lysed in lysis buffer (20 m*M* Tris/HCl, pH 8, 1% Triton X-100, 137 m*M* NaCl, 1.5 m*M* $MgCl_2$, 10% glycerol, 1 m*M* EGTA, 50 m*M* NaF, 1 m*M* Na_3VO_4, 10 m*M* β-glycerophosphate, 1 m*M* phenylmethylsulfonyl fluoride [PMSF], 1 μg/ml leupeptin, and 1 μg/ml aprotinin). Protein concentration of the lysate was determined by the Bradford method. The sample was analyzed by SDS-PAGE and immunoblotting with antibodies to Rb, $p21^{Cip1}$, $p27^{Kip1}$, and actin according to manufacturers' instructions.

Statistical Analysis. Student's *t* test was used to determine the statistical significance between treatment groups in each experiment. Differences were considered statistically significant at a value of $P < 0.05$.

Results

Growth Inhibition by HA. To determine the cellular effect of HA on fibroblasts, we treated human foreskin fibroblasts (HFF) with increasing HA concentrations, and examined their growth kinetics. The untreated control displayed an exponential growth pattern. On the contrary, the growth rates of HFF cells incubated with HA for only 36 hr were significantly reduced (Fig. 1A). Such effect was conspicuous at the HA concentration as low as 10 μg/ml, and became more prominent at higher doses of HA; the cell number in cultures treated with 100 μg/ml HA for 36 hr was about 50% lower than that of control (Fig. 1B). Prolonged HA treatment (for up to 72 hr) resulted in even greater growth suppressive effect (Fig. 1A).

The HA-induced growth stagnation in HFF cells was characterized by the cell cycle arrest at G1 phase. After 36 hr of treatment with HA (from 10 to 100 μg/ml), the cell cycle distribution showed an accumulation of G1 cells in a dose-dependent manner (Table I); at the highest concentration used, HA caused a notable increase in G1 cells (86.31% ± 0.41% for the 100 μg/ml group vs 54.63% ± 2.56% for the untreated control), and the corresponding decreases in S phase cells (5.96% ± 0.83% for the 100 μg/ml group vs 28.18% ± 0.63% for the untreated control) and G2/M phase cells (7.73% ± 0.42% for the 100 μg/ml group vs 17.22% ± 1.93% for the untreated control). This was well correlated with the dwindling proliferation rate of HA-treated HFF cells.

G1 progression is controlled through activity of retinoblastoma (Rb) protein, which exists in hypo- and hyperphosphorylated forms. The active, hypophosphorylated, but not the hyperphosphorylated, form binds to and inhibits E2F transcription factors necessary for G1 to S transition (39, 40). Upon HA treatment, the level of hyperphosphorylated Rb decreased in dose-dependent manner (Fig. 1C). Rb is phosphorylated by cyclin-dependent kinase activity, which is in turn regulated in part by Cdk inhibitors such as $p21^{Cip1}$ and $p27^{Kip1}$ (41–45). Expression of both proteins was elevated in HA-treated HFF cells when compared with the untreated control (Fig. 1C). Such results are consistent with the growth kinetics of HA-treated cells.

Prolonged HA Treatment-Induced Apoptosis. Intriguingly, growth curves revealed significant decreases in cell number when the HA treatment was extended from 72 to 120 hr (Fig. 1A). Such reduction in cell number showed dose dependence, and was due to an increased level of cell death. The dying cells exhibited convoluted outline and membrane blebbings, both of which are typical of apoptotic cells (data not shown).

The extent of apoptosis was quantified by the following approaches. TUNEL labeling of the free DNA ends formed by fragmentation of genomic DNA, followed by flow cytometric analysis, gives a reliable means for quantification of apoptosis (46, 47). Prolonged HA treatment caused an increase in mean relative fluorescence, indicating incorpo-

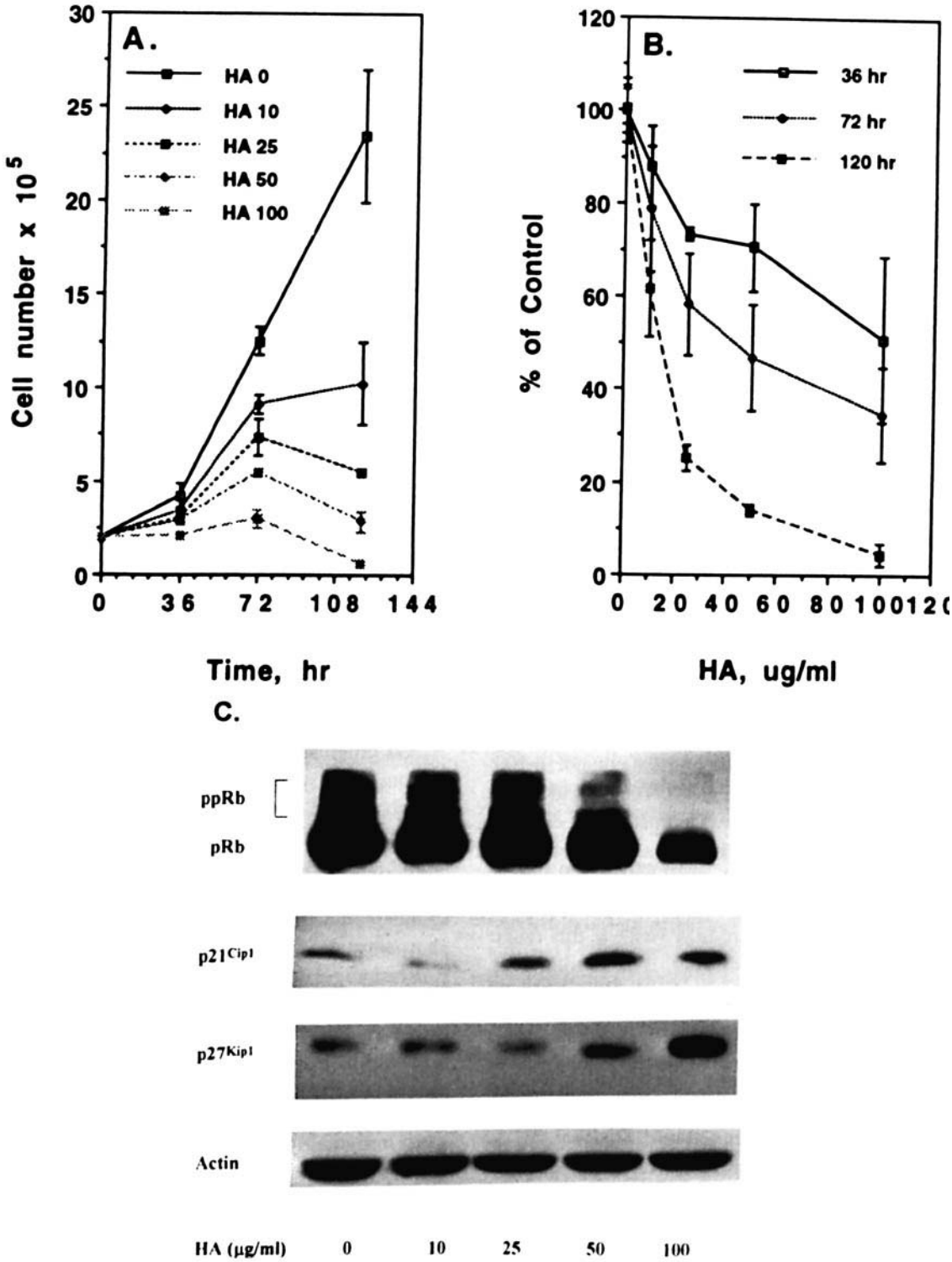

Figure 1. Effect of HA on growth kinetics of HFF. (A) About 2 x 10^5 cells were seeded overnight, and were then treated with 0, 10, 25, 50, or 100 μg/ml HA. Cell number was determined 36, 72, and 120 hr after addition of HA. (B) Growth inhibitory effect of HA on HFF cells showed dose dependence. About 2 x 10^5 cells were treated with the indicated concentrations of HA. The cell number was determined 36, 72, and 120 hr afterward, and is expressed relative to that of untreated control. Results are presented as mean ± SD of five determinations. (C) Expression of cell cycle-related proteins, Rb, $p21^{Cip1}$ and $p27^{Kip1}$, in HA-treated HFF cells. Cells were treated with indicated concentrations of HA, and harvested 36 hr later. Cell lysates were separated by SDS-PAGE and analyzed with indicated antibodies by Western blotting. It should be noted that the anti-Rb antibody recognizes both the hypo- (pRb) and hyperphosphorylated (ppRb) forms. The results shown here are representative of at least three experiments.

Table I. Effect of HA and Vitamin E on Cell Cycle of HFF Cells

HA concentration (μg/ml)	Percentage of cells in different phases					
	G1 phase		S phase		G2/M phase	
	−Vitamin E	+Vitamin E	−Vitamin E	+Vitamin E	−Vitamin E	+Vitamin E
0	54.63 ± 2.56	52.89 ± 4.12	28.18 ± 0.63	33.43 ± 4.74	17.22 ± 1.93	13.68 ± 5.36
10	68.47 ± 1.86	65.27 ± 2.71	15.45 ± 0.71	20.56 ± 1.88	16.09 ± 2.55	13.68 ± 0.34
25	73.47 ± 1.42	69.44 ± 3.11	13.90 ± 2.21	20.10 ± 0.85	12.59 ± 0.80	10.29 ± 2.81
50	79.30 ± 1.89	73.88 ± 1.03[a]	10.71 ± 2.56	17.20 ± 0.14[a]	9.94 ± 0.75	8.91 ± 0.89
100	86.31 ± 0.41	80.17 ± 1.43[b]	5.96 ± 0.83	11.52 ± 0.57[b]	7.73 ± 0.42	8.32 ± 0.85

Note. After 30 min preincubation with (+) or without (−) vitamin E (200 μg/ml), HFF cells were treated with the indicated concentrations of HA for 36 hr. They were then harvested for cell cycle analysis as described in the "Materials and Methods" section. The percentages of cells in different phases of cell cycle were quantified using *Modfit* software (Becton Dickinson, CA). Data are mean ± SD from three independent experiments.

[a] $P < 0.05$.

[b] $P < 0.005$ vs. the corresponding group without vitamin E pretreatment.

ration of fluorescein-dUTP onto ends of nuclear DNA fragments in apoptotic cells (Fig. 2A). Apoptosis was barely detectable in cells treated for 36 hr at all the HA concentrations; it became significant in the experimental groups receiving 72 hr of treatment with 10 μg/ml HA (Fig. 2B). Additional increases in incubation time and/or HA concentration drastically elevated the percentage of TUNEL-positive cells: 120 hr of treatment caused significant level of apoptosis at HA concentrations ranging from 10 to 100 μg/ml.

The appearance of cells with a low DNA stainability (sub-G1 fraction) in cell population has been considered as a marker of apoptosis (48). The sub-G1 fraction varies with treatment time and HA concentration in a pattern similar to that of TUNEL-positive cells. Over 40% of cells underwent apoptosis in response to 120 hr of treatment with 100 μg/ml of HA, whereas only insignificant level of apoptosis was observed in cells receiving 36 hr of treatment at all the HA concentrations used.

Increased Oxidative Stress and 8-OHdG Formation in HA-Treated HFF Cells. We previously demonstrated that HA induces oxidative damages to erythrocytes (20). To determine whether HA also elicited oxidative stress in nucleated cells, we loaded HFF cells with dichlorofluorescin, and examined them after 24 hr of HA treatment. H_2DCF has been used in a number of studies to monitor overall oxidative stress in single cells (49–51). Once oxidized, the leuco form H_2DCF is converted into fluorescent DCF. If an oxidative insult occurs, these dye-loaded cells will take on a greenish appearance under fluorescence microscope. As shown in Figure 3, increased fluorescence of DCF, and hence increased oxidative stress, was observed in HA-treated HFF cells, whereas only a very low level (close to the background in unstained cells) of fluorescence was detected in untreated control. Of note, the fluorescence level increased with HA concentration (Fig. 3, F–J). Experiments with another fluorogenic dye dihydrorhodamine 123 gave similar results (data not shown). Moreover, as compared with the untreated control (Fig. 3A), a

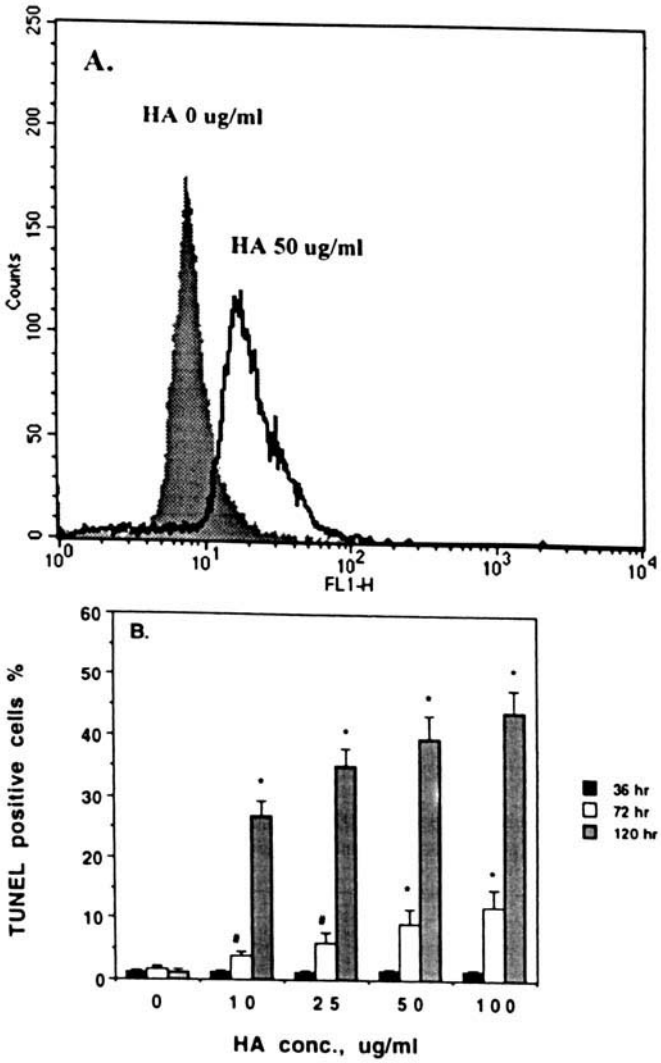

Figure 2. Quantification of the extent of apoptosis in HFF cells by TUNEL assay. (A) HFF cells were treated with varying concentrations of HA, and the level of apoptosis was determined 120 hr later by TUNEL assay and flow cytometric analysis. Representative histograms of HFF cells treated with 0 and 50 μg/ml of HA are shown here. (B) The extent of apoptosis with varying HA concentrations for HFF cells is shown here. Results are expressed as mean ± SD from three experiments. #$P < 0.05$; *$P < 0.005$ vs. the untreated control.

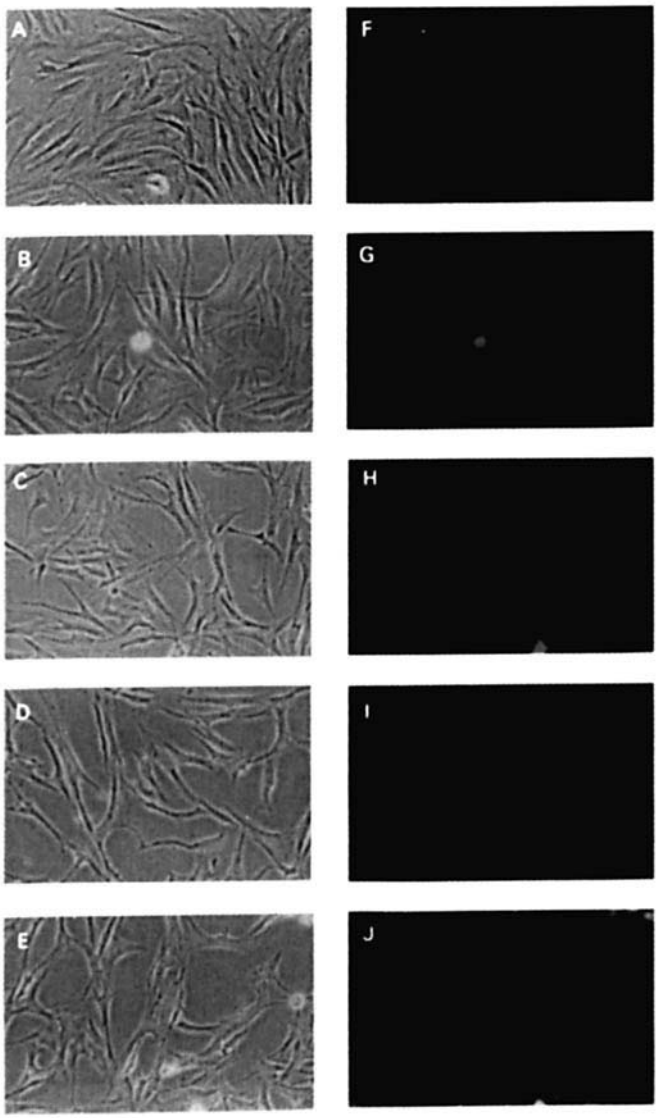

Figure 3. H_2DCF staining for reactive oxygen species in HA-treated HFF cells. HFF cells were treated with 0 μg/ml (A and F), 10 μg/ml (B and G), 25 μg/ml (C and H), 50 μg/ml (D and I), and 100 μg/ml (E and J) of HA for 24 hr. After a change of medium, the cells were loaded with 10 μM H_2DCFDA for 5 min. The samples were examined under inverted (A–E) and fluorescence microscope (F–J). The representative photographs shown here are taken from one out of five experiments (original magnification: x200).

number of HA-treated cells showed slender morphology with greatly extended, spike-like cellular processes (Fig. 3, D and E), which was indicative of a stressful intracellular milieu.

It is plausible that HA-induced oxidative stress causes severe damage to macromolecules, in particular DNA, leading to growth arrest and cell death. Therefore, we measured the extent of oxidative DNA damage in HFF cells treated in different ways. The level of 8-OHdG, a reliable marker for assessment of oxidative DNA damage, was detected using HPLC-electrochemical method (30, 52). Figure 4 shows representative chromatograms of 8-OHdG and total deoxyguanosine in DNA from cells treated with or without 50 μg/ml HA. The magnitude of oxidative DNA damage induced by HA was considerable (Table II). Treatment of cells with 100 μg/ml for 120 hr produced about 57 8-OHdG adducts per 10^6 dG molecules, an over 4.5-fold increase as compared with the untreated control. It was evident that 8-OHdG formation increased with the HA dosage and duration of treatment. The 8-OHdG/dG ratios for cells incubated with 50 and 100 μg/ml for 72 hr increased by nearly 2- and 3-fold, respectively; after an additional 48-hr treatment, the corresponding values were 3.15 and 4.68 times that of control.

Prevention of HA-Induced 8-OHdG Formation and Cellular Changes by Vitamin E. Vitamin E, a potent lipid peroxyl radical scavenger, has been shown to reduce oxidant-induced nuclear damages (53). Accordingly, we examined the possibility of using vitamin E to prevent the deleterious effect of HA. Pretreatment of HFF cells with vitamin E greatly diminished the HA-induced 8-OHdG adduct formation (Table II). Thirty minutes of incubation with 200 μg/ml vitamin E could reduce the 8-OHdG/dG ratios by more than 50% in experimental groups treated with 100 μg/ml HA for 72 and 120 hr.

Reduction in 8-OHdG/dG ratio was paralleled by abatement of the growth inhibitory effect of HA. As shown in Figure 5, the cell numbers in the vitamin E- and HA-treated groups were significantly higher than those in HA-treated groups. After 36 hr of incubation with 50 μg/ml HA, the cell number was about 54.65% ± 5.37% of the control without HA treatment; however, with vitamin E pretreatment, this increased to 85.40% ± 7.20% of the control (Fig. 5A). A similar protective effect of vitamin E was observed for 72 and 120 hr of treatment (Fig. 5, B and C). Consistent with this, vitamin E ameliorated the G1 arrest imposed by HA: the percentage of G1 cells was significantly lower in the group treated with vitamin E and 100 μg/ml HA than in the one with HA alone (Table I). More important, vitamin E abolished the HA-induced apoptosis (Fig. 6). At whatever concentration, HA failed to induce apoptosis in the presence of vitamin E. Apparently, vitamin E was so potent as to completely prevent apoptosis under the condition that usually led over 40% of cells to demise.

Discussion

Previous studies have implicated dysfunction of endothelial cells in the arteriosclerotic changes associated with Blackfoot disease (17, 21, 22). However, this does not fully explain the persistence of chronic ulcers at the extremities of patients. The pathogenesis of chronic ulcers is multifactorial (54). There has not been any study examining the effect of HA on human fibroblast, a crucial player in wound repair. Here, our results demonstrate that HA instigated growth arrest and apoptosis in fibroblasts. These changes were associated with increased oxidative stress, and could be prevented, to a large extent, by vitamin E treatment.

Apparently, there is an intimate relationship between HA and ROS. Being a polyphenolic compound, HA has been shown to generate ROS such as superoxide anion (55). It is believed that the di-, trihydroxylphenolic, and quinone

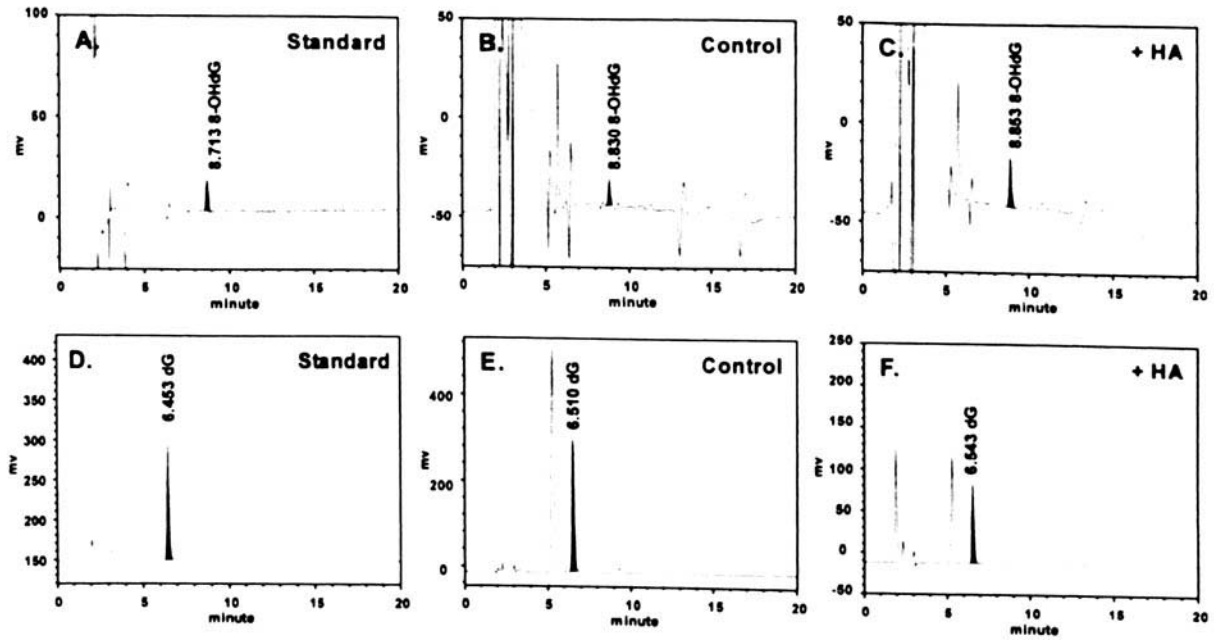

Figure 4. HPLC analysis of 8-OHdG and dG in DNA of HA-treated HFF cells. Chromatograms for 8-OHdG (A) and dG (D) standards are shown here. HFF cells were untreated (B and E) or treated with 50 μg/ml of HA for 72 hr (C and F). Cellular DNA was isolated and processed as described in the "Materials and Methods" section for quantification of 8-OHdG (B and C) and dG (E and F). The amounts of 8-OHdG and dG were calculated by measuring the area under the corresponding peaks in chromatograms. These representative chromatograms are taken from one out of three experiments.

Table II. HA-Induced Formation of 8-OHdG in HFF Cells

HA concentration (μg/ml)	Level of 8-OHdG in cellular DNA (8-OHdG/10^6 dG)					
	36-hr incubation		72-hr incubation		120-hr incubation	
	−Vitamin E	+Vitamin E	−Vitamin E	+Vitamin E	−Vitamin E	+Vitamin E
0	11.02 ± 3.07	9.21 ± 1.03	12.77 ± 1.78	9.67 ± 1.25	12.22 ± 1.41	11.23 ± 1.70
25	13.15 ± 2.02	10.69 ± 1.85	16.71 ± 4.10	11.08 ± 0.81	23.44 ± 4.87	14.35 ± 1.40
50	19.45 ± 2.41	14.77 ± 2.45	23.26 ± 3.89	16.40 ± 2.68[a]	38.55 ± 7.34	21.10 ± 1.12[a]
100	25.61 ± 4.25	14.69 ± 2.51[a]	37.25 ± 4.71	15.87 ± 3.78[b]	57.20 ± 2.95	24.17 ± 0.78[b]

Note. After 30 min preincubation with (+) or without (−) vitamin E (200 μg/ml), HFF cells were treated with the indicated concentrations of HA for 36, 72, or 120 hr. They were then harvested for DNA extraction and HPLC analysis, as described in the "Materials and Methods" section. The amount of 8-OHdG is expressed as the number of 8-OHdG per 1 × 10^6 dG (8-OHdG/10^6 dG). Data are shown as mean ± SD from three independent experiments.

[a] $P < 0.05$.

[b] $P < 0.005$ vs. the group without vitamin E pretreatment.

structures in HA can give rise to stable benzosemiquinone radicals that may directly attack cellular components or indirectly do so through generation of secondary free radicals. In erythrocytes, it causes a depletion of glutathione and several antioxidant enzymes (20). Clinically, the levels of serum lipid peroxides are significantly higher in patients with Blackfoot disease (56). Our results demonstrate that addition of HA caused a dose-dependent increase in DCF fluorescence in H_2DCF-loaded cells (Fig. 3). Moreover, HA significantly increased 8-OHdG adduct formation in cellular DNA (Table II). These findings clearly show that HA generates oxidative stress and inflicts oxidative damages on human fibroblasts. It follows that preincubation with a chain-breaking antioxidant, vitamin E, was able to reduce the oxidative DNA damage (Table II). Indeed, these data are consistent with previous findings that HA can induce lipid peroxidation in erythrocytes (20), chondrocytes (57), and endothelial cells (58). Change in cell morphology is known to be a consequence of oxidative stress. Oxidants can modulate cytoskeletal proteins, resulting in actin cytoskeleton reorganization and changes in cell shape (59). A number of HFF cells receiving short-term HA treatment assumed a slender appearance with spike-like processes, instead of a normal flat morphology (Fig. 3). The mechanism for such change remains obscure. The ROS may effect through the direct alteration of the redox state of cytoskeletal proteins such as actin and its regulators (59–61), or may indirectly do so via other signaling pathways (62–64). More important, such morphological change and the accompanying change in cell-matrix contact may represent major alteration in cell physiology, for instance, a switch from growth to quiescence (65).

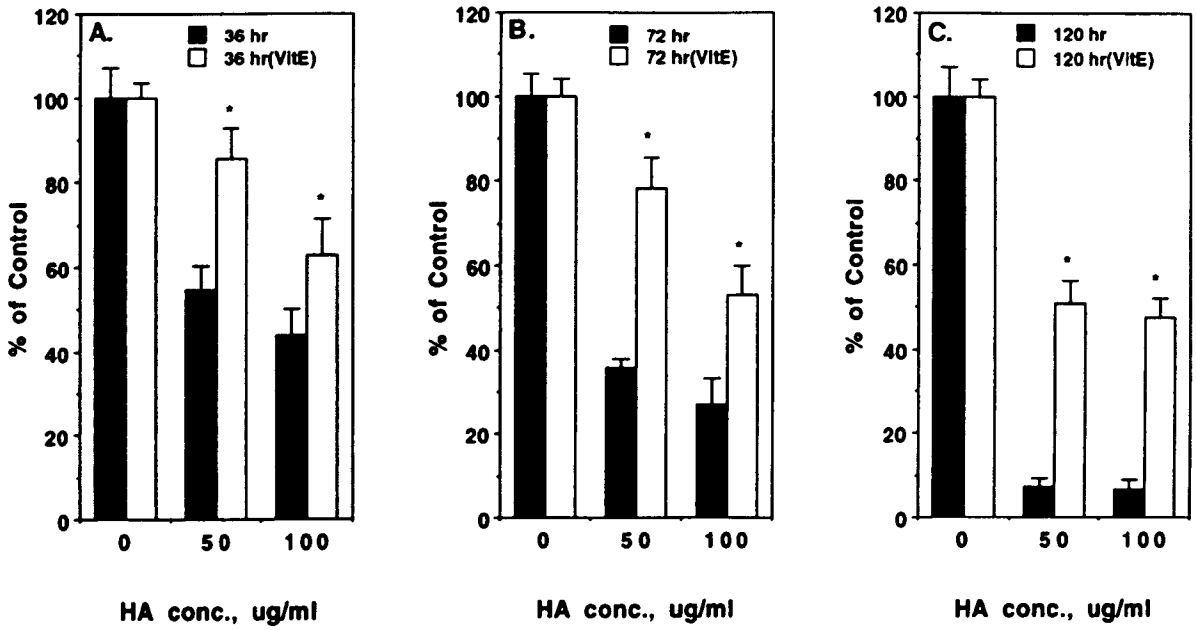

Figure 5. Growth inhibitory effect of HA was alleviated by vitamin E. HFF cells were incubated with or without 200 μg/ml vitamin E for 30 min, and then treated with the indicated concentrations of HA for 36 hr (A), 72 hr (B), or 120 hr (C). The cell number in each treatment group is expressed relative to that of control without HA treatment, which is assigned 100%. The data are presented as mean ± SD of four separate experiments. $^*P < 0.005$ vs. the corresponding group without vitamin E pretreatment.

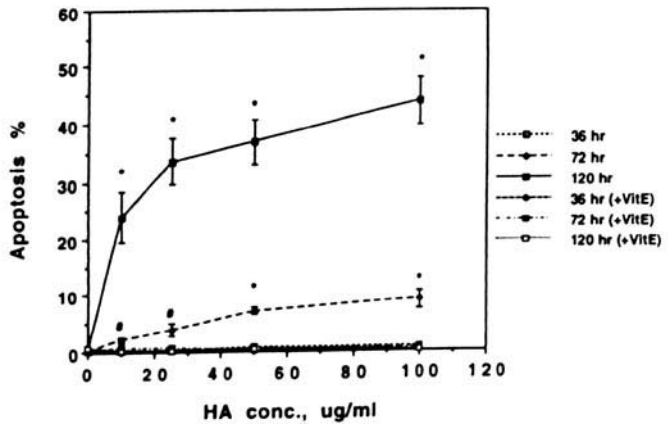

Figure 6. Vitamin E-protected HFF cells from HA-induced apoptosis. HFF cells were incubated with or without 200 μg/ml vitamin E for 30 min, and then treated with the indicated concentrations of HA for 36, 72, or 120 hr. The extent of apoptosis was subsequently measured by PI staining and flow cytometric analysis. The data are presented as mean ± SD from four separate experiments. $\#P < 0.05$; $^*P < 0.005$ vs. the corresponding group with vitamin E pretreatment.

Free radicals have been implicated in regulating cell growth and death (66). HFF cells exhibited a diminished capacity to grow upon exposure to HA (Fig. 1). They underwent cell cycle arrest in G1 phase (Table I). In agreement with this, cyclin-dependent kinase inhibitors, $p21^{Cip1}$ and $p27^{Kip1}$, the expression of which was associated with G1 arrest (41–45), accumulated in HA-treated HFF cells (Fig. 1C). This was accompanied by reduction in the level of Rb phosphorylation (Fig. 1C). As mentioned earlier, cell geometry is closely related to growth control (67, 68). The change in cell morphology, together with a reduction in the area of cell-matrix contact, correlated well with their diminished proliferation and/or survival. Long-term treatment of cells with HA resulted in apoptosis (Figs. 2 and 6). A similar finding on endothelial cells has been recently reported (69). Vitamin E significantly relieved HA-treated HFF cells of growth inhibition, and completely blocked their apoptosis (Figs. 5 and 6), suggesting the involvement of ROS in these processes. Our results have several implications. First, HA induces G1 growth arrest as a protective mechanism. Cell cycle checkpoints are believed to allow time for cells to repair oxidative damage to macromolecules, in particular DNA, before their re-entering the cell cycle and completing such events as DNA synthesis and mitosis. In this way, genome integrity is preserved (70). Second, HA elicits apoptosis as an alternative mechanism to deal with irreparably damaged cells. Persistent oxidative stress during long-term HA incubation may cause overloading of repair system. The level of damage then exceeds the threshold required to trigger apoptosis. Furthermore, the complete blockage of HA-induced cell death by vitamin E suggests the involvement of lipid peroxidation in initiation or execution phase of apoptosis (71).

The finding that HA induced growth cessation and apoptosis in fibroblasts sheds light into the pathogenesis of Blackfoot disease. Chronic ulcers result from complex interaction between various factors, for instance, arterial insufficiency, inflammation, and neuropathy (19, 72). Our previous studies have shown that HA causes injuries to endothelial cells (21, 22), and erythrocytes (20), possibly accounting for the reduced blood supply to the extremities of Blackfoot patients. However, the picture is far from complete. Chronic wounds also represent the inability of epithelial cells and fibroblasts to carry out healing process

(23–27). Being a critical player in wound healing, dermal fibroblasts proliferate actively during formation of granulation tissue (23–27). The present study clearly demonstrates that HA inflicts serious oxidative damage on human dermal fibroblasts, and impairs their ability to grow. This probably explains, in part, the persistence of chronic ulcers in Blackfoot patients.

Increased oxidative DNA damage in HA-treated cells is intriguing in cancer biology. It has been known for a long time that the humic substances isolated from artesian well water in Blackfoot endemic region are mutagenic (73). There are high incidences of skin, liver, lung, and bladder cancer in the same region (9, 74). Elevated 8-OHdG adduct formation in HA-treated cells provides a connection between HA and carcinogenesis. 8-Hydroxy-2'-deoxyguanosine is mutagenic itself: depending on its conformation, 8-OHdG can pair with dC or dA, and if unrepaired properly, causes G:C to T:A mutation (75, 76). As a marker of oxidative DNA damage, increased 8-OHdG formation indicates an overt oxidative attack on DNA. In addition to 8-OHdG, other base oxidation products, adducts, and even DNA strand breaks may be formed (77–82). The strand break lesions frequently cause various kinds of chromosomal aberrations, such as translocation and deletion (83, 84). Interestingly, there exist increased frequencies of chromosomal aberrations in lymphocytes isolated from cancer patients who inhabit the Blackfoot endemic area (85). Our findings also suggest that HA may be an etiological factor of cancer, and that HA-induced oxidative damage can be an underlying mechanism of carcinogenesis in the Blackfoot endemic region.

The current study clearly demonstrates that HA induces oxidative stress in dermal fibroblasts, leading to growth arrest and apoptosis. This suggests that HA-induced dysfunction of fibroblasts is implicated in the pathogenesis of Blackfoot disease. Nonetheless, more studies should be conducted before we apply our findings to the more complex clinical situation. Intriguingly, that vitamin E can reduce HA-elicited oxidative raises the possibility of using antioxidants as therapeutic intervention of Blackfoot disease.

1. Hartenstein R. Sludge decomposition and stabilization. Science **212**:743–749, 1981.
2. Stevenson FJ. Geochemistry of soil humic substances. In: Aiken GR, McKnight DM, Wershaw RL, Maccarthy P, Eds. Humic Substances in Soil, Sediment and Water. New York: John Wiley & Sons, pp13–52, 1985.
3. Stevenson IL, Schnitzer M. Transmission electron microscopy of extracted fulvic and humic acids. Soil Sci **113**:179–185, 1982.
4. Gamble DS, Schnitzer M. The chemistry of fulvic acid and its reaction with metal ions. In: Singer P, Ed. Trace Metals and Metal-Organic Interactions. Ann Arbor, MI: Ann Arbor Science, pp225–340, 1974.
5. Thurman EM, Malcolm RL. Structural study of humic substances: new approaches and methods. In: Christman RF, Gjessing ET, Eds. Aquatic and Terrestrial Humic Materials. Ann Arbor, MI: Ann Arbor Science Publishers, pp1–35, 1983.
6. Gaitan E, Jolly RL, Lee NE, Lindsay RJ, Cooksey RC, Hill JR, Kelly K. Phthalate ester: possible progoitrogens in water supply of a Colombia district with endemic goiter. J Am Chem Soc **23**:175–178, 1983.
7. Cookesy RC, Gaitan E, Lindsay RJ, Hill JR, Keely K. Humic substances, a possible source of environmental goitrogens. Org Geochem **8**:77–80, 1985.
8. Gaitan E, Medina TA, Zia MS. Goiter prevalence and bacterial contamination of water supply. J Clin Endocrinol Metab **51**:957–961, 1980.
9. Lu FJ, Guo HR, Chiangs HS, Hong CL. Relationships between the fluorescent intensity of well water and the incidence rate of bladder cancer. J Chinese Oncol Soc **2**:14–23, 1986.
10. Lu FJ, Yamamura Y, Yamauchi H. Studies on fluorescent compounds in water of a well in Blackfoot disease endemic areas in Taiwan: humic substances. J Formos Med Assoc **87**:66–75, 1988.
11. Lu FJ. Blackfoot disease: arsenic or humic acid? Lancet **336**:115–116, 1990.
12. Lu FJ. Fluorescent humic substances and Blackfoot disease in Taiwan. Appl Organometal Chem **4**:191–195, 1990.
13. Zhai SS, Kimbrough RD, Meng B, Han JY, Levoid M, Hou X, Yin XN. Kashin-Beck disease: a cross-sectional study in seven villages in the People's Republic of China. J Toxicol Environ Health **30**:239–259, 1990.
14. Huang TS, Lu FJ, Tsai CW, Chopra IJ. Effect of humic acids on thyroidal function. J Endocrinol Invest **17**:787–791, 1994.
15. Lu FJ, Liu TM. Fluorescent compounds in drinking water of Blackfoot disease endemic areas: animal experimental model. J Formos Med Assoc **85**:352–358, 1986.
16. Huang TS, Lu FJ, Tsai CW. Tissue distribution of absorbed humic acids. Environ Geochem Health **17**:1–4, 1995.
17. Kuo ZB, Chen MZ. A clinical therapy of Blackfoot disease. J Formos Med Assoc **68**:275–289, 1969.
18. Lu FJ, Huang TS, Lin YS, Pang VF, Lin SY. Peripheral vasculopathy in rats induced by humic acids. Appl Organometal Chem **8**:223–228, 1994.
19. Sarkar PK, Ballantyne S. Management of leg ulcers. Postgrad Med J **76**:674–682, 2000.
20. Cheng ML, Ho HY, Chiu DTY, Lu FJ. Humic acid-mediated oxidative damages to human erythrocytes: a possible mechanism leading to anemia in Blackfoot disease. Free Radic Biol Med **27**:470–477, 1999.
21. Chiu HC, Shin SR, Lu FJ, Yang HL. Stimulation of endothelin production in cultured human endothelial cells by fluorescent compounds associated with Blackfoot disease. Thromb Res **63**:139–151, 1993.
22. Chiu HC, Shin SH, Lu FJ. The fluorescent compounds from drinking water and the vascular disorders of Blackfoot disease. FASEB J **A523**:884, 1991.
23. Singer AJ, Clark RAF. Cutaneous wound healing. New Engl J Med **341**:738–746, 1999.
24. Werner S, Smola H, Liao X, Longaker MT, Krieg T, Hofschneider PH, Williams LT. The function of KGF in morphogenesis of epithelium and re-epithelialization of wounds. Science **266**:819–822, 1994.
25. Regan MC, Kirk SJ, Wasserkrug HL, Barbul A. The wound environment as a regulator of fibroblast phenotype. J Surg Res **50**:442–448, 1991.
26. Gabbiani G. Evolution and clinical implications of the myofibroblast concept. Cardiovasc Res **38**:545–548, 1998.
27. Powell DW, Mifflin RC, Valentich JD, Crowe SE, Saada JI, West AB. Myofibroblasts. I. Paracrine cells important in health and disease. Am J Physiol **277**:C1–C9, 1999.
28. Kasai H, Nishimura S. Hydroxylation of deoxyguanosine at the C-8 position by ascorbic acid and other reducing agents. Nucleic Acids Res **12**:2137–2145, 1984.
29. Cheng KC, Cahill DS, Kasai H, Nishimura S, Loeb LA. 8-Hydroxyguanine, an abundant form of oxidative DNA damage, causes G→T and A→C substitutions. J Biol Chem **267**:166–172, 1992.
30. Helbock HJ, Beckman KB, Shigenaga MK, Walter PB, Woodall AA, Yeo HC, Ames BN. DNA oxidation matters: the HPLC-

electrochemical detection assay of 8-oxo-deoxy-guanosine and 8-oxo-guanine. Proc Natl Acad Sci USA **95**:288–293, 1998.
31. Schnitzers MT. Organic matter characterization. In: Page AL, Ed. Methods of Soil Analysis, Part 2, Chemical and Microbiological Properties. New York, NY: Academic Press, pp581–594, 1982.
32. Ho HY, Cheng ML, Lu FJ, Chou YH, Stern A, Liang CM, Chiu DTY. Enhanced oxidative stress and accelerated cellular senescence in glucose-6-phosphate dehydrogenase (G6PD)-deficient human fibroblasts. Free Radic Biol Med **29**:156–169, 2000.
33. Cheng ML, Ho HY, Liang CM, Chou YH, Stern A, Lu FJ, Chiu DTY. Cellular glucose-6-phosphate dehydrogenase (G6PD) status modulates the effects of nitric oxide (NO) on human foreskin fibroblasts. FEBS Lett **475**:257–262, 2000.
34. Gorczyca W, Gong J, Ardelt B, Traganos F, Darzynkiewicz Z. The cell cycle related difference in susceptibility of HL-60 cells to apoptosis induced by various antitumor agents. Cancer Res **53**:3186–3192, 1993.
35. Royall JA, Ischiropoulos H. Evaluation of 2',7'-dichlorofluorescin and dihydrorhodamine 123 as fluorescent probes for intracellular H_2O_2in cultured endothelial cells. Arch Biochem Biophy **302**:348–355, 1993.
36. Haugland RP. Probes for reactive oxygen species, including nitric oxide. In: Haugland RP, Spence MTZ, Ed. Handbook of Fluorescent Probes and Research Chemicals. Oregon: Molecular Probes Inc., pp483–502, 1996.
37. Loft S, Poulsen HE. Markers of oxidative damage to DNA: antioxidants and molecular damage. Method Enzymol **300**:166–184, 1999.
38. Watanabe N, Miura S, Zeki S, Ishii H. Hepatocellular oxidative DNA injury induced by macrophage-derived nitric oxide. Free Radic Biol Med **30**:1019–1028, 2001.
39. Weinberg RA. The retinoblastoma protein and cell cycle control. Cell **81**:323–330, 1995.
40. Chen PL, Scully P, Shew JY, Wang JY, Lee WH. Phosphorylation of the retinoblastoma gene product is modulated during the cell cycle and cellular differentiation. Cell **58**:1193–1198, 1989.
41. Shackelford RE, Kaufman WK, Paules RS. Oxidative stress and cell cycle checkpoint function. Free Radic Biol Med **28**:1387–1404, 2000.
42. Vidal A, Koff A. Cell-cycle inhibitors: three families united by a common cause. Gene **247**:1–15, 2000.
43. Sherr CJ, Roberts JM. CDK inhibitors: positive and negative regulators of G1-phase progression. Genes Dev **13**:1501–1512, 1999.
44. Harper JW, Adami GR, Wei N, Keyomarsi K, Elledge SJ. The p21 Cdk-interacting protein Cip1 is a potent inhibitor of G1 cyclin-dependent kinases. Cell **75**:805–816, 1993.
45. Polyak K, Kato JY, Solomon MJ, Sherr CJ, Massague J, Roberts JM, Koff A. $p27^{Kip1}$, a cyclin-Cdk inhibitor, links transforming growth factor β and contact inhibition to cell cycle arrest. Genes Dev **8**:9–22, 1994.
46. Raghuram N, Fortenberry JD, Owens ML, Brown LA. Effect of exogenous nitric oxide and hyperoxia on lung fibroblast viability and DNA fragmentation. Biochem Biophys Res Commun **262**:685–691, 1999.
47. Darzynkiewicz Z, Li X, Gong J, Hara S, Traganos F. Analysis of cell death by flow cytometry. In: Studzinski GP, Ed. Cell Growth and Apoptosis. Newark, NJ: IRL Press, pp143–167, 1995.
48. Nicoletti I, Migliorati G, Pagliacci MC, Grignani F, Riccardi C. A rapid and simple method for measuring thymocyte apoptosis by propidium iodide. J Immunol Methods **139**:271–279, 1991.
49. Bass DA, Parce JW, Dechatelet LR, Szejda P, Seeds MC, Thomas M. Flow cytometric studies of oxidative product formation by neutrophils: a graded response to membrane stimulation. J Immunol **130**:1910–1917, 1983.
50. Hempel SL, Buettner GR, O'Malley YQ, Wessels DA, Flaherty DM. Dihydrofluorescein diacetate is superior for detecting intracellular oxidants: comparison with 2', 7'-dichlorodihydrofluorescein diacetate, 5 (and 6)-carboxy-2', 7'-dichlorodihydrofluorescein diacetate, and dihydrorhodamine 123. Free Radic Biol Med **27**:146–159, 1999.
51. Zhu H, Bannenberg GL, Moldeus P, Shertzer HG. Oxidation pathways for the intracellular probe 2', 7'-dichlorofluorescein. Arch Toxicol **68**:582–587, 1994.
52. Helbock HJ, Beckman KB, Ames BN. 8-Hydroxydeoxyguanosine and 8-hydroxyguanine as biomarkers of oxidative DNA damage. Methods Enzymol **300**:156–166, 1999.
53. Claycombe KJ, Meydani SN. Vitamin E and genome stability. Mutat Res **475**:37–44, 2001.
54. Falanga V, Grinell F, Gilchrest B, Maddox YT, Moshell A. Workshop on the pathogenesis of chronic wounds. J Invest Dermatol **102**:125–127, 1994.
55. Vaughan D, Ord G. An *in vitro* effect of soil organic matter fractions and synthetic humic acids on the generation of superoxide radicals. Plant Soil **66**:113–116, 1982.
56. Lu FJ, Lu JY. Serum lipid peroxides in patients with Blackfoot disease. J Formos Med Assoc **86**:76–80, 1987.
57. Liang HJ, Tsai CL, Chen PQ, Lu FJ. Oxidative injury induced by synthetic humic acid polymer and monomer in cultured rabbit articular chondrocytes. Life Sci **65**:1163–1173, 1999.
58. Gau RJ, Yang HL, Suen JL, Lu FJ. Induction of oxidative stress by humic acid through increasing intracellular iron: a possible mechanism leading to atherothrombotic vascular disorder in Blackfoot disease. Biochem Biophys Res Comm **283**:743–749, 2001.
59. Dalle-Donne I, Rossi R, Milzani A, DiSimplicio P, Colombo R. The actin cytoskeleton response to oxidants: from small heat shock protein phosphorylation to changes in the redox state of actin itself. Free Radic Biol Med **31**:1624–1632, 2001.
60. Rokutan K, Johnston RB Jr, Kawai K. Oxidative stress induces *S*-thiolation of specific proteins in cultured gastric mucosal cells. Am J Physiol **266**:G247–G254, 1994.
61. Dalledonne I, Milzani A, Colombo R. H_2O_2-treated actin: assembly and polymer interactions with cross-linking proteins. Biophys J **69**:2710–2719, 1995.
62. Huot J, Houle F, Marceau F, Landry J. Oxidative stress-induced actin reorganization mediated by the p38 mitogen-activated protein kinase/heat shock protein 27 pathway in vascular endothelial cells. Circ Res **80**:383–392, 1997.
63. Song SH, Lee KH, Kang MS, Lee YJ. Role of paxillin in metabolic oxidative stress-induced cytoskeletal reorganization: involvement of SAPK signal transduction pathway and PTP-PEST gene expression. Free Radic Biol Med **29**:61–70, 2000.
64. Hinshaw DB, Burger JM, Armstrong BC, Hyslop PA. Mechanism of endothelial cell shape change in oxidant injury. J Surg Res **46**:339–349, 1989.
65. Huang S, Ingber DE. Shape-dependent control of cell growth, differentiation, and apoptosis: switching between attractors in cell regulatory networks. Exp Cell Res **261**:91–103, 2000.
66. Droge W. Free radicals in the physiological control of cell function. Physiol Rev **82**:47–95, 2002.
67. Huang S, Ingber DE. The structural and mechanical complexity of cell-growth control. Nat Cell Biol **1**:E131–E138, 1999.
68. Chen CS, Mrksich M, Huang S, Whitesides GM, Ingber DE. Geometric control of cell life and death. Science **276**:1425–1428, 1997.
69. Hseu YC, Huang HW, Wang SY, Chen HY, Lu FJ, Gau RJ, Yang HL. Humic acid induces apoptosis in human endothelial cells. Toxicol Appl Pharmacol **182**:34–43, 2002.
70. Norbury CJ, Hickson ID. Cellular responses to DNA damage. Annu Rev Pharmacol Toxicol **41**:367–401, 2001.
71. Chandra J, Samali A, Orrenius S. Triggering and modulation of apoptosis by oxidative stress. Free Radic Biol Med **29**:323–333, 2000.
72. Stadelmann WK, Digenis AG, Tobin GR. Physiology and healing dynamics of chronic cutaneous wounds. Am J Surg **176**:26S–38S, 1998.
73. Lu FJ. Contribution of the fluorescent substances existing in well water of the Blackfoot disease endemic area in the Chia-Nan area to environmental toxicology research in Taiwan. J Formos Med Assoc **88**:76–83, 1989.

74. Lu FJ, Hong CL, Lu MF, Shimizu H. Mutagenicity of drinking well water. Bull Environ Contam Toxicol **51**:545–550, 1993.
75. Shibutani S, Takeshita M, Grollman AP. Insertion of specific bases during DNA synthesis past the oxidation-damaged base 8-oxodG. Nature **349**:431–434, 1991.
76. Le Page F, Guy A, Cadet J, Sarasin A, Gentil A. Repair and mutagenic potency of 8-oxoG:A and 8-oxoG:C base pairs in mammalian cells. Nucleic Acids Res **26**:1276–1281, 1998.
77. Dizdaroglu M. Oxidative damage to DNA in mammalian chromatin. Mutat Res **275**:331–342, 1992.
78. Nilsen H, Krokan HE. Base excision repair in a network of defense and tolerance. Carcinogenesis **22**:987–998, 2001.
79. Marnett LJ. Oxyradicals and DNA damage. Carcinogenesis **21**:361–370, 2000.
80. Burcham PC. Genotoxic lipid peroxidation products: their DNA damaging properties and role in formation of endogenous DNA adducts. Mutagenesis **13**:287–305, 1998.
81. Lee SH, Oe T, Blair IA. Vitamin C-induced decomposition of lipid hydroperoxides to endogenous genotoxins. Science **292**:2083–2086, 2001.
82. Mello-Filho AC, Meneghini R. *In vivo* formation of single-strand breaks in DNA by hydrogen peroxide is mediated by the Haber-Weiss reaction. Biochim Biophys Acta **781**:56–63, 1984.
83. Hoeijmakers JH. Genome maintenance mechanisms for preventing cancer. Nature **411**:366–374, 2001.
84. Memisoglu A, Samson L. Base excision repair in yeast and mammals. Mutat Res **451**:39–51, 2000.
85. Liou SH, Lung JC, Chen YH, Yang T, Hsieh LL, Chen CJ, Wu TN. Increased chromosome-type chromosome aberration frequencies as biomarkers of cancer risk in a Blackfoot endemic area. Cancer Res **59**:1481–1484, 1999.